Myosin I Contributes to the Generation of Resting Cortical Tension

Jianwu Dai,* H. Ping Ting-Beall,# Robert M. Hochmuth,# Michael P. Sheetz,* and Margaret A. Titus*
*Department of Cell Biology, Duke University Medical Center, Durham, North Carolina 27710, and #Department of Mechanical Engineering and Materials Sciences, Duke University, Durham, North Carolina 27708 USA

ABSTRACT The amoeboid myosin I's are required for cellular cortical functions such as pseudopod formation and macropinocytosis, as demonstrated by the finding that *Dictyostelium* cells overexpressing or lacking one or more of these actin-based motors are defective in these processes. Defects in these processes are concomitant with changes in the actin-filled cortex of various *Dictyostelium* myosin I mutants. Given that the amoeboid myosin I's possess both actin- and membrane-binding domains, the mutant phenotypes could be due to alterations in the generation and/or regulation of cell cortical tension. This has been directly tested by analyzing mutant *Dictyostelium* that either lacks or overexpresses various myosin I's, using micropipette aspiration techniques. *Dictyostelium* cells lacking only one myosin I have normal levels of cortical tension. However, myosin I double mutants have significantly reduced (50%) cortical tension, and those that mildly overexpress an amoeboid myosin I exhibit increased cortical tension. Treatment of either type of mutant with the lectin concanavalin A (ConA) that cross-links surface receptors results in significant increases in cortical tension, suggesting that the contractile activity of these myosin I's is not controlled by this stimulus. These results demonstrate that myosin I's work cooperatively to contribute substantially to the generation of resting cortical tension that is required for efficient cell migration and macropinocytosis.

INTRODUCTION

The amoeboid myosin I's are a conserved class of actin-based motor proteins found in a variety of organisms and cell types (Mooseker and Cheney, 1995). Originally discovered in the free-living soil amoeba *Acanthamoeba castellanii* and subsequently identified in a wide range of cell types (Pollard and Korn, 1973; Coluccio, 1997), they have been thought to play a role in powering pseudopod extension or vesicle transport (Pollard et al., 1991). Myosin I's comprise a single heavy chain of 110–130 kDa and one to six low-molecular-mass light chains (Mooseker and Cheney, 1995). The tail domain of the amoeboid myosin I's can be divided into three distinct domains (Pollard et al., 1991). The first domain, rich in basic amino acids, is the polybasic domain. This domain has been shown to be capable of high-affinity binding directly to stripped plasma membranes as well as to anionic phospholipid vesicles in vitro (Adams and Pollard, 1989; Miyata et al., 1989; Doberstein and Pollard, 1992). This polybasic domain is followed by a region rich in the amino acids glycine, proline, and alanine (or serine or glutamate), referred to as the GPA domain. In vitro studies have shown that this region serves as an ATP-insensitive actin-binding site (Lynch et al., 1986; Doberstein and Pollard, 1992; Jung and Hammer, 1994; Rosenfeld and Rener, 1994). Finally, there is a *src* homology 3 (SH3) domain present at or near the extreme C-terminus. SH3 domains have been identified in a number of proteins that are associated with both the plasma membrane and the actin cytoskeleton. Although the precise role of the myosin I SH3 domain is unknown, it has been shown to be essential for *Dictyostelium* myosin I function in vivo (Novak and Titus, 1998), and a specific *Acanthamoeba* myosin I SH3 domain binding protein has been identified (Xu et al., 1997). The nature of the various myosin I tail domains is consistent with the proposed roles for myosin I's.

Dictyostelium expresses multiple myosin I's (Uyeda and Titus, 1997), as do many different cell types (Mooseker and Cheney, 1995). MyoB, C, and D are typical amoeboid myosin I's with a 125–135-kDa heavy chain, whereas myoA, E, and F are "short" myosin I's whose tail regions are composed solely of a polybasic domain (Uyeda and Titus, 1997). Analysis of *Dictyostelium* mutants lacking either myoA or myoB revealed that they exhibit similar phenotypic abnormalities (Jung and Hammer, 1990; Wessels et al., 1991; Titus et al., 1993). These two single mutants are each delayed in streaming, exhibiting a 50% decreased instantaneous velocity and an increased frequency of turning (Jung and Hammer, 1990; Wessels et al., 1991; Titus et al., 1993; Peterson et al., 1995). The slowed motility correlates with defects in pseudopod formation. The $myoA^-$ and $myoB^-$ mutants both extend twice as many pseudopodia as wild-type cells, at half the rate of wild-type cells (Wessels et al., 1991, 1996; Titus et al., 1993). A detailed analysis of pseudopod extension in the $myoA^-$ mutant revealed that it extended a greater overall proportion of pseudopodia in contact with the substratum and that these cells extended more than one psuedopod at a time, in contrast to wild-type cells (Wessels et al., 1996). Finally, the $myoA^-$ and $myoB^-$ mutants both secrete abnormally high levels of lysosomal enzymes (Temesvari et al., 1996).

Received for publication 13 October 1998 and in final form 5 May 1999.

Address reprint requests to Dr. Margaret A. Titus, Department of Genetics, Cell Biology, and Development, University of Minnesota, 4-102 Owre Hall, 321 Church St. SE, Minneapolis, MN 55455. Tel.: 612-625-8498; Fax: 612-624-8118; E-mail: titus@lenti.med.umn.edu.

Dr. Dai's present address is Hematology Division, Brigham and Women's Hospital, LMRC 301, 221 Longwood Ave., Boston, MA 02115.

0006-3495/99/08/1168/09 $2.00

Taken together, these results suggested that myoA and myoB play highly similar if not identical roles in controlling actin-dependent cortical processes required for the proper extension of psuedopodia and regulated secretion of lysosomal enzymes.

Deletion of two *Dictyostelium* myosin I's (*myoA*$^-$/*B*$^-$, *myoB*$^-$/*C*$^-$, and *myoB*$^-$/*D*$^-$) results in additional defects in cellular function while not further compromising cellular motility (Novak et al., 1995; Jung et al., 1996). The myosin I double mutants have significant defects in macropinocytosis (i.e., non-receptor-mediated fluid-phase uptake; Novak et al., 1995; Jung et al., 1996). Where examined, the double mutants also transiently extend an excess of actin-rich crowns (Novak et al., 1995) that have been implicated in macropinocytosis (Hacker et al., 1997). Together with the analysis of the single mutant phenotypes, these findings suggested that the myosin I's participate in several distinct cortical functions such as pseudopod extension and macropinocytosis.

Dictyostelium cells that mildly overexpress myoB (myoB$^+$ cells) also exhibit significant defects in macropinocytosis and cell migration (Novak and Titus, 1997). The myoB$^+$ cells accumulate more F-actin and myoB than found in wild-type cells at their periphery and have a less polarized, hypercontracted appearance. These findings suggested that the excess myosin I contributed to a constriction of the cortex that resulted in an inability to properly manipulate macropinocytic crowns and pseudopodia.

The combined results of the myosin I null and overexpression mutants indicates that myosin I may provide a contractile force at the cortex that is required for the efficient manipulation of extended actin-filled plasma membrane projections, either by participating in their retraction or by contributing to the optimal cortical tension required for general function. Most cells have a continuous cortical shell of actin with a thickness on the order of 0.05–0.1 μm beneath the plasma membrane, and this cortex is under constant isotropic contraction. In the resting or passive state, the cell surface area is determined by the contractile tension of the cortex (Zhelev et al., 1994). Alterations of cell cortex composition or activity would therefore be expected to affect cell surface dynamics. Previous analysis of myosin I deletion or overexpression mutants in *Dictyostelium* revealed that these cells exhibit changes in cell surface dynamics of actin-filled structures (such as the formation of excess pseudopodia and other surface protrusions in the case of deletion mutants and the inhibition of the formation of these same structures in overexpresssion mutants; Novak et al., 1995; Novak and Titus, 1997). These gross changes in the number and activity of the various actin-filled structures are likely to be caused by alterations in the resting cortical tension in these cells due to change in the composition or activity of the cortex. Several methods have been employed for measuring cortical tension, and among these micropipette aspiration (Evans and Yeung, 1989) permits the rapid and accurate analysis of the cortical tension of large numbers of cells. This method has been employed to evaluate directly the contribution of myosin I to the generation of resting cortical tension by measuring the cortical tension of a number of different strains of *Dictyostelium* that either lack or overexpress various myosin I's.

MATERIALS AND METHODS

Maintenance of strains

The *Dictyostelium* parental Ax3 (referred to throughout as wild-type), *myoA*$^-$, *myoB*$^-$, *myoC*$^-$, *myoA*$^-$/*B*$^-$, *myoB*$^-$/*C*$^-$, myoB$^+$, and myoC$^+$ strains were all maintained in HL5, either in suspension or on a substrate, by standard methods (Spudich, 1982). A list of the strains used for this study is presented in Table 1. Suspension cultures were grown in 100 ml HL5 while shaking at 240 rpm. Substrate cultures were grown in 10 ml HL5 on bacteriological plastic. The *myoA*$^-$, *myoA*$^-$/*B*$^-$, *myoB*$^-$/*C*$^-$, myoB$^+$, and myoC$^+$ cultures were maintained in the presence of 10 μg/ml G418 (Geneticin; Gibco BRL, Gaithersburg, MD).

Construction of plasmids

The first step in the generation of a *myoC* overexpression plasmid was to engineer a restriction enzyme site at the 5′ end of the *myoC* gene so that it could be placed under the control of an exogenous promoter. A polymerase chain reaction (PCR) employing both the MYC26 primer (5′ GCCGAATTCATGAGATCTGCACAACAAAAACCAGAATGG 3′) introduced the unique *Eco*RI site immediately preceding the start ATG, and the CSEQ24 antisense primer (5′ GATTTGATGAACTAGCTC 3′, nucleotides 398–415) to generate a 415-bp product. This fragment was incubated with T4 DNA polymerase in the presence of excess deoxynucleotides to fill in any overhanging ends, digested with *Eco*RI, and ligated to *Eco*RI/*Sma*I-digested pGEM7 (Promega, Madison, WI). The sequence of the resulting plasmid, pDTc16, was then confirmed to ensure that there were no errors introduced by the PCR.

The pDTc16 plasmid was then transformed into *dam*$^-$ bacteria and digested first with *Hind*III, and then partially digested with *Bcl*I. The longer plasmid fragment (3.1 kb) was gel-purified. The *myoC*-containing 5B plasmid that encompassed the entire *myoC* gene, including 0.3 kb of 5′ and 0.4 kb of 3′ noncoding sequences (a gift of Dr. John Hammer, III, National Institutes of Health), was digested with *Bcl*I and *Hind*III, and the 1.9-kb fragment was isolated and then ligated to the digested pDTc16, resulting in pDTc17. pDTc17 was then digested with *Xho*I (a site in the polylinker upstream of the ATG) and treated with Klenow enzyme in the presence of excess deoxynucleotide to fill in the overhanging nucleotides. The 0.3-kb actin 15 promoter was released from pDRH (Faix et al., 1992), treated with the Klenow enzyme in the presence of excess deoxynucleotide to fill in the overhanging nucleotides, and gel-purified. The actin 15 promoter fragment was then ligated to pDTc17, and a clone containing the promoter in the correct orientation was selected and named pDTc18.

The 3′ region of the *myoC* gene was isolated from the pDTc1 plasmid (Peterson et al., 1995) by digestion with *Cla*I and *Sma*I and subsequent gel purification of the 3.6-kb fragment. pDTc18 was digested first with *Hind*III, treated with Klenow enzyme in the presence of excess de-

TABLE 1 Myosin I mutant strains employed for this study

Colloquial name	Strain name	Reference
myoA$^-$	HTD1-12	Titus et al. (1993)
myoB$^-$	HTD4-3	Novak et al. (1995)
myoC$^-$	HTD3-1	Peterson et al. (1995)
myoA$^-$/B$^-$	HTD5-2	Novak et al. (1995)
myoB$^-$/C$^-$	HTD6-1	Novak et al. (1995)
S332A	—	Novak and Titus (1998)
myoB$^+$	HTD8	Novak and Titus (1997)
myoC$^+$	HTD14-1	This study

oxynucleotides to fill in the overhanging nucleotides, and then digested with *Cla*I. The 4.7-kb 5′ fragment of the *myoC* gene was then ligated to the 3.6-kb *Cla*I/*Sma*I pDTc1 fragment, resulting in pDTc19. Finally, pDTc19 was digested with *Xba*I and *Bam*HI, and the 5.7-kb fragment was gel-purified and then ligated to *Xba*I-/Bam HI-digested pLittle, resulting in pDTc20, the myoC overexpression plasmid. pLittle is a Ddp1-based *Dictyostelium* extrachromosomal shuttle vector derived from pBIG (Patterson and Spudich, 1995) that carries the gene for neomycin transferase, conferring resistance on G418.

Dictyostelium transformations

The transformation of *Dictyostelium* was performed following a slightly modified version (Kuspa and Loomis, 1992) of the original protocol (Howard et al., 1988). Ten micrograms of pDTc20 plasmid was transformed into log-phase Ax3 cells by electroporation, and the cells were allowed to recover overnight in HL5. The cells were then diluted by 1:10 into HL5 containing 10 μg/ml G418, and the medium was exchanged every third day. Neomycin-resistant colonies were visible by 9 days. Twenty independent clones from each transformation were picked and transferred into individual 10-ml plates and subjected to analysis once grown to confluence.

The amount of myoC heavy chain expressed by any individual clone was determined by quantitative Western blot analysis (Novak and Titus, 1997), using a rabbit polyclonal antibody generated against the purified myoC heavy chain (Lee and Côté, 1993), which was generously provided to us by Dr. Graham P. Côté (Queens University, Ontario, Canada). A total of three independent transformants, named HTD14–1, HTD14–2, and HTD14–3, respectively, were analyzed in detail. The results of a single clone, HTD14–1, whose behavior was representative of all of the clones examined, are presented here. This strain is colloquially referred to as myoC$^+$ throughout the paper.

Functional assays

The pinocytosis rate was measured by analyzing the intensity of tetramethylrhodamine isothiocyanate-dextran (TRITC-dextran) internalized by the cells over the course of 2 h, using a slightly modified version of a published assay (Rauchenberger et al., 1997). After the collection and trypan blue quenching of a sample, it was immediately placed on ice until all of the time points were collected. A fluorescence-activated cell sorter (FACS) was used to measure the relative fluorescence intensity of each sample. The laser wavelength was tuned to 530 nm, and the signals were collected at about 570 nm. A total of 10^5 cells were measured for each sample.

The streaming assay was performed as previously described (Jung and Hammer, 1990; Peterson et al., 1995). Streaming cells were observed on a Leica DMIL inverted phase microscope, using a 10× or 20× objective. Images were captured with Adobe Photoshop 3.0, using a Hamamatsu color chilled 3CCD camera (model C5810).

Cell size estimation

We obtained the information from cell forward light scattering (FSC) by using a FACS (McNeil et al., 1985). The FSC value largely depends on the cell size (McNeil et al., 1985). A total of 10^5 cells were measured from each sample. This method allowed us to estimate the size of cells of a large population.

Measurement of cell cortical tension with micropipette aspiration

Several different methods have been used to study cell cortical tension (Evans and Yeung, 1989; Pasternak et al., 1989; Egelhoff et al., 1996). Among them, micropipette aspiration has been shown to be an effective and precise one. The precondition for the cortical tension to be calculated from the micropipette manipulation experiment is that the cell can be treated by the so-called cortical shell-liquid core or liquid drop model (Evans and Yeung, 1989). To test this, a cell is aspired into a micropipette to form a hemispherical projection inside the micropipette. If the suction pressure is higher than the threshold or "critical" pressure required to form a hemispherical projection, the cell continuously flows into the pipette. If the pressure is reduced to the threshold pressure during the initial phase of entry, flow stops. When the cell is released from the pipette, the cell slowly recovers its original spherical shape. This behavior corresponds to that of a liquid drop with a constant surface tension.

To measure the cell cortical tension, the radius of the spherical cell (R_c) and the internal radius of the micropipette tip (R_p) were measured. The radii of the pipettes are in the range of 3–3.5 μm, and cell radii were in the range of 5–7 μm. Then the cell was deformed by aspirating part of the cell into the pipette, and the critical pressure (ΔP) required to form a hemispherical projection into the pipette was measured. To determine ΔP, an aspiration pressure was set to a small value and increased slowly until the cell formed a hemispherical projection and remained stationary in the pipette. To be able to use the theory to calculate the cortical tension, using data from the micropipette experiment, the "cortical shell-liquid core" theory was used. This model includes the assumption that the core (cytoplasm) will not resist a static deformation (i.e., it is a liquid), and the cell possess a constant surface (cortical) tension. Thus the cortical tension (T_c) can be calculated with the following equation (Evans and Yeung, 1989):

$$\Delta P = 2T_c(1/R_p - 1/R_c).$$

RESULTS

Overexpression of the myoC heavy chain

The goal of our work was to measure the cortical tension of several different types of *Dictyostelium* myosin I mutants. Although a number of myosin I null mutants were already available, only a single characterized overexpression strain was available (Novak and Titus, 1997). A second overexpression strain, one that expressed an excess of the myoC heavy chain, was first generated and characterized to give us a second example of this type of *Dictyostelium* myosin I mutant to test.

A myoC overexpression vector (Fig. 1 *A*) similar to that used for the overexpression of the myoB heavy chain (Novak and Titus, 1997) was generated. The pDTc20 vector carried the full-length *myoC* gene under the control of the exogenous actin15 promoter, the Neo gene, and Ddp1 sequences for low-copy number extrachromosomal maintenance of the plasmid in *Dictyostelium*. Electrotransformation of this plasmid into Ax3 cells, followed by selection in G418, resulted in numerous colonies. These were screened for the myoC heavy chain levels by quantitative immunoblot analysis. The three clones analyzed were found to mildly overexpress the myoC heavy chain, with values ranging from 1.7- to 1.9-fold (Fig. 1 *B*). Three independent clones were selected and found to behave identically in the assays performed. The detailed analysis of only one clone of myoC$^+$ cells, HTD14–1, is presented here.

Analysis of the myoC$^+$ phenotype

The most striking phenotypes observed in the myoB$^+$ cells were a marked decrease in pinocytosis and a delay in

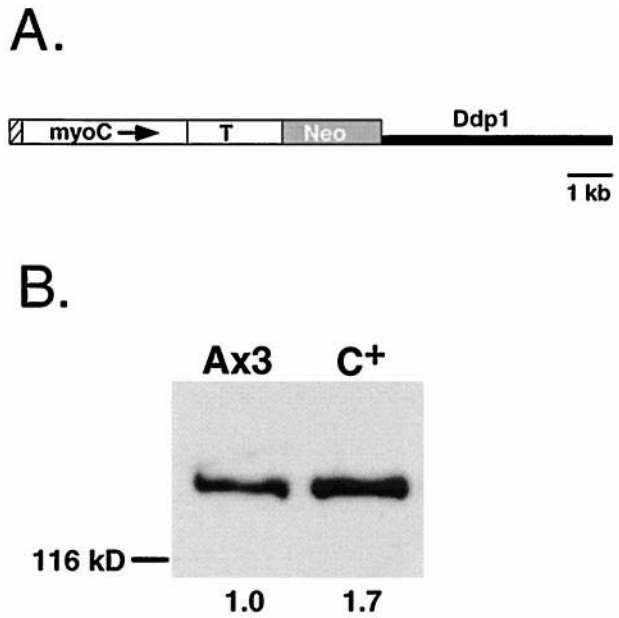

FIGURE 1 Increased amounts of myoC heavy chain are expressed in the myoC$^+$ strain. (*A*) Diagram of the pDTc20 myoC overexpression vector. The pLittle-based plasmid pDTc20 contains the 0.3-kb actin 15 promoter (*hatched box*) upstream of the full-length 3.75-kb *myoC* gene (myoC) and 2.0 kb of the 3′ noncoding sequence (T). The arrow represents the direction of *myoC* transcription. The *myoC* gene is immediately adjacent to the 2.2-kb neomycin resistance cassette (*gray box labeled Neo*), whose transcription is driven by the actin 6 promoter. This is followed by the 4.9-kb Ddp1 extrachromosomal replication element. The 2.9-kb pBluescript vector backbone is not illustrated in this diagram. (*B*) Quantitative immunoblot analysis of the myoC$^+$ strain. Shown is a region of a Western blot of the parental Ax3 strain and the myoC$^+$ (C$^+$) mutant. The numbers below each lane indicate the relative amount of 137-kDa myoC heavy chain expressed by each of the two cell types. Shown to the left is the position of the 116-kDa molecular mass marker.

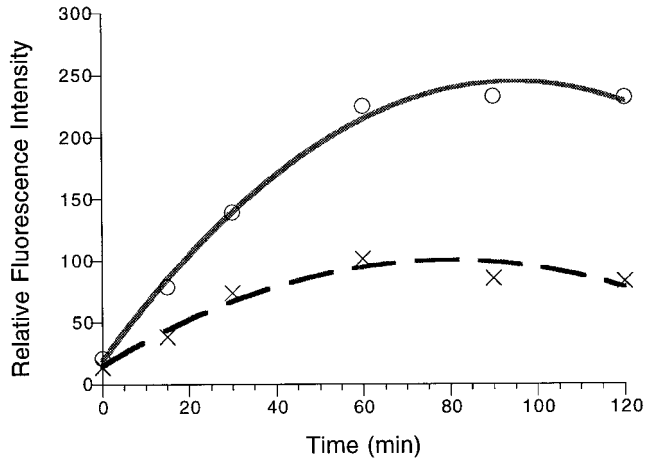

FIGURE 2 Pinocytosis is reduced in the myoC$^+$ strain. The uptake of TRITC-dextran (relative fluorescence) over the course of 2 h is shown for Ax3 (○, ——) and myoC$^+$ cells (×, – – –). The points shown are the average of three independent measurements.

streaming (Novak and Titus, 1997). The myoC$^+$ cells were first analyzed for their ability to take up the fluid-phase marker, TRITC-dextran. They exhibited a significant decrease in pinocytic activity (Fig. 2). The overall extent of inhibition was significant but not as severe as observed for the myoB$^+$ cells, 60% versus 80% (Novak and Titus, 1997). The decreased pinocytic rate was accompanied by a slower rate of growth in suspension. The Ax3 cells doubled their cell density every 8–9 h, whereas the myoC$^+$ cell number doubled every 12–15 h.

The ability of the myoC$^+$ cells to undergo directed and efficient cell migration was tested by monitoring streaming, the aggregation of amoebae into mounds, in submerged culture (Jung and Hammer, 1990). The Ax3 cells initiated streaming 8 h after being transferred into starvation medium and formed mounds by 14 h, as has previously been shown (Novak et al., 1995; Peterson et al., 1995; Novak and Titus, 1997). In contrast, the myoC$^+$ strain exhibited a delay and did not initiate streaming until ~13 h after the onset of starvation (Fig. 3). This delay is similar to that observed for myoB$^+$ cells and is longer than observed for either the *myoA*$^-$ or *myoB*$^-$ single mutants that begin to stream at 10 h under the same conditions (Peterson et al., 1995; Novak and Titus, 1997) .

Liquid-like behavior of *Dictyostelium* cells and decrease in cortical tension of myosin I null mutants

The technique of micropipette aspiration has been used for measuring cortical tension of several cell types (Evans and Yeung, 1989; Needham and Hochmuth, 1990; Tsai et al., 1994; Zhelev and Hochmuth, 1995). The theory that allows us to calculate the cortical tension from the micropipette manipulation experiment is the cortical shell-liquid core or "liquid drop" model (Yeung and Evans, 1989). When *Dictyostelium* cells were aspired into pipettes with a pressure higher than the threshold pressure, they formed extensions inside the pipets and continuously flowed into the pipettes; when the pressure was equal to the threshold pressure, flow ceased. When the cells were released from the pipette, they slowly recovered (see Fig. 4). This liquid-like response indicates that *Dictyostelium* cells behave much like a highly viscous liquid drop with a persistent cortical tension. However, the extremely large value of the threshold pressure indicates that *Dictyostelium* cells have a high value for the cortical tension compared with that of neutrophils and other granulocytes (Evans and Yeung, 1989; Zhelev and Hochmuth, 1995).

The resting cortical tension of cells has been found to be dependent on the actin cytoskeleton (Tsai et al., 1994; Ting-Beall et al., 1995), and given the altered cortical properties of many of the *Dictyostelium* myosin I mutants, it was suspected that their cortical tension might differ from that of wild-type cells (Novak et al., 1995). The cortical tension of several different myosin I null mutants was measured and compared to that of wild type. It should be noted that these

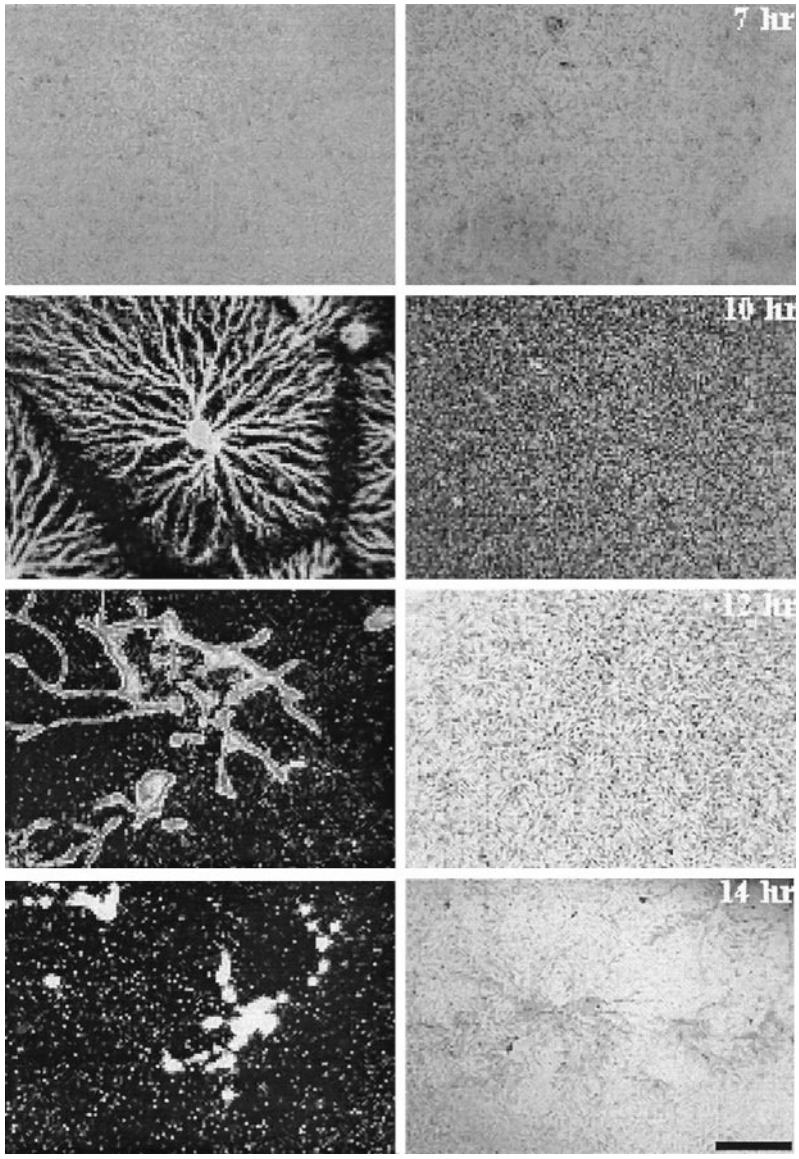

FIGURE 3 The myoC$^+$ cells are delayed in streaming. Shown is a series of images taken during the course of streaming in submerged culture. The progress of parallel cultures of streaming Ax3 (*left column*) and myoC$^+$ (*right column*) cells at different time points (7, 10, 12, and 14 h) is presented. Scale bar = 2 mm

measurements were carried out on cells suspended in liquid medium and not attached to a substrate (see Fig. 5).

The Ax3 cells were found to have a basal cortical tension of 1.50 dyn/cm (Fig. 6). This value is comparable to that measured for Ax4 (4.1 dyne/cm) and JH10 (3.2 dyn/cm) cells adhering to a substrate, as determined by two completely different methods, a cell poker and a glass needle (Pasternak et al., 1989; Egelhoff et al., 1996). Thus the three methods are in relative agreement and the results obtained by micropipette aspiration can be compared to those obtained by other methods.

The single myosin I mutants, *myoA*$^-$, *myoB*$^-$, and *myoC*$^-$ cells, exhibited cortical tension similar to that of the wild-type cells, ranging from 1.25 to 1.6 dyn/cm (Fig. 6). In contrast, the *myoA*$^-$/*B*$^-$ and *myoB*$^-$/*C*$^-$ double mutants exhibited lower cortical tension values than either the wild-type or single mutants (0.6 and 0.7 dyn/cm, respectively; Fig. 6). These values were similar to those found for the *Dictyostelium* myosin II null mutants measured under similar conditions, 0.5 dyn/cm (Fig. 6). The finding that the single mutants have normal levels of cortical tension while the double mutants have reduced cortical tension suggests that the myosin I's cooperatively contribute to the overall cortical tension of *Dictyostelium* cells but do not make large individual contributions.

The protozoan amoeboid myosin I's require phosphorylation at a single serine or threonine residue in the motor domain, near the actin-binding site, for full activity (Brzeska and Korn, 1996). Mutation of this site from serine to alanaine has been shown to inactivate myosin I function both in vivo and in vitro (Novak and Titus, 1997; Novak and Titus, 1998; Wang et al., 1998). The resting cortical tension of a myosin I mutant strain lacking myoA and expressing a myoB heavy chain with the consensus phosphorylation site changed from serine to alanine (S332A; Novak and Titus, 1998) was examined to test the role of motor activity in cortical tension generation. The measured tension for the S332A strain (~0.6 dyne/cm) was indistinguishable from

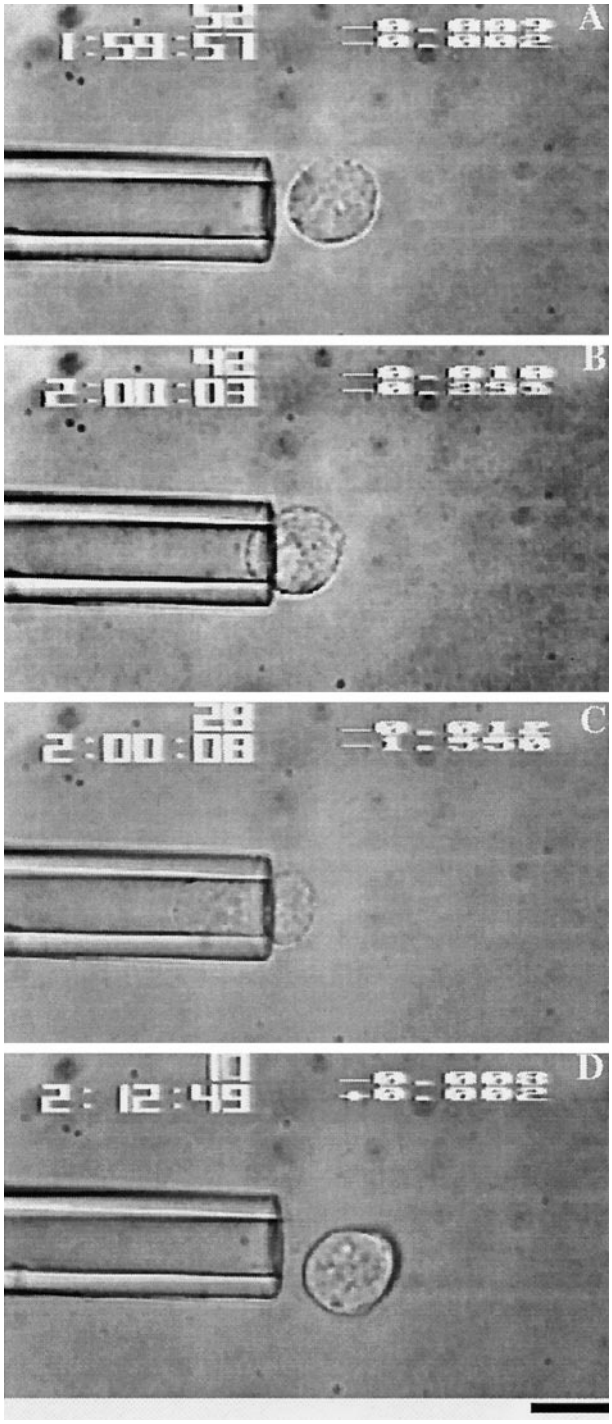

FIGURE 4 Liquid-like response of a *Dictyostelium* cell to micropipette suction. The pictures show that a suspended *Dictyostelium* cell (*A*) formed a hemispherical projection inside a pipette under threshold pressure (*B*). When the pressure was increased, the cell flowed into the pipette (*C*). When released from the pipette, the cell slowly recovered its spherical shape (*D*). Scale bar = 8 μm

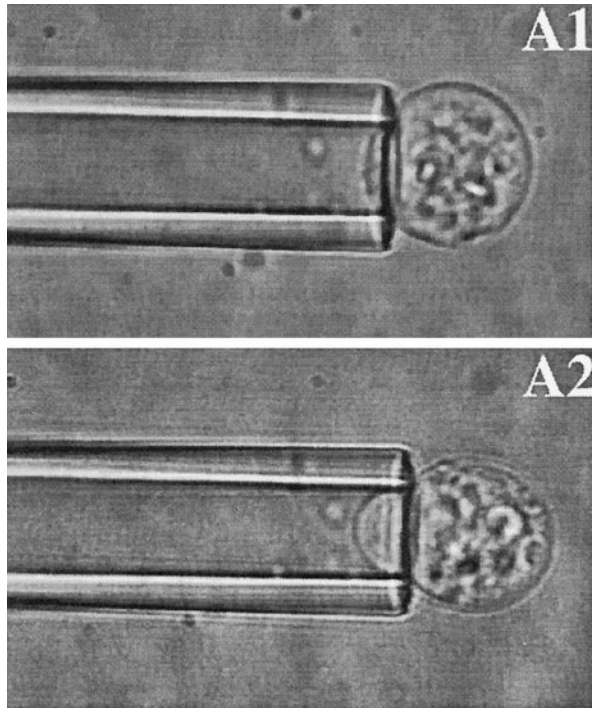

FIGURE 5 Pictures of pipette during a cortical tension experiment. A1 and A2 show that a *Dictyostelium* cell was deformed by a pipette for the cortical tension measurement. Scale bar = 4 μm.

that of the parental *myoA*$^-$/*B*$^-$ double mutant (Fig. 6), indicating that myosin I motor activity is required for generating cortical tension.

The determination of the cortical tension requires that the diameter of the individual cell be known. During the course of these measurements it appeared that the overall diameter of the double mutants was smaller than that of either the wild type or myosin I single mutants. This was examined directly for a large population of cells by FACS. The forward light scattering value of the cell measured by FACS has been shown to largely depend on the size of cells (McNeil et al., 1985). The overall size of the single mutants appeared to be somewhat smaller than that of the Ax3 cells;

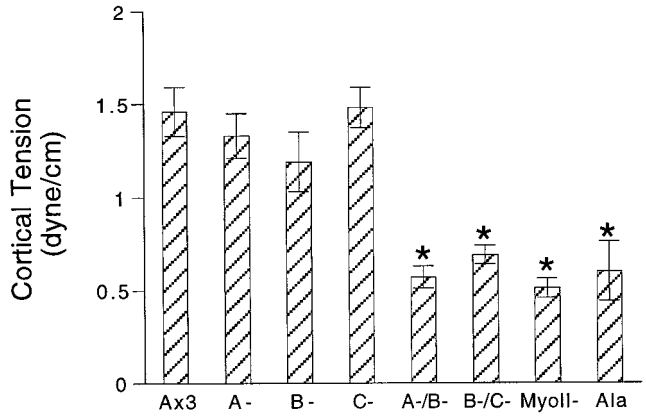

FIGURE 6 The cortical tension of myosin I null cells is decreased. Shown are the results of the cortical tension measurement for myosin I single and double mutants and the S332A strain (Ala). Also shown is the cortical tension for the myosin II null mutant. The average results ± standard errors of 20–50 cells in each group are shown. The * above individual bars indicates that there is a statistically significant difference between this group and the wild-type control.

both double mutants were found to have an even smaller size (Fig. 7).

Increase in cortical tension of the myosin I overexpression strains

The appearance and behavior of the myosin I overexpression strains suggested that increasing the amount of myosin I present in the cell resulted in hypercontraction of the cortex (Novak and Titus, 1997). The cortical tension of both the myoB$^+$ and myoC$^+$ cells was directly measured by micropipette aspiration. The cortical tension of the myoB$^+$ cells, expressing an approximately threefold excess of the myoB heavy chain, was found to be 2.5 dyn/cm (Fig. 8). This is significantly higher than that of the wild-type cells. Similarly, the myoC$^+$ strain was found to have cortical tension values of ~1.9 dyn/cm. These results indicate that the excess myosin I heavy chain in these different overexpression strains creates an increase in the overall cortical tension (Fig. 8).

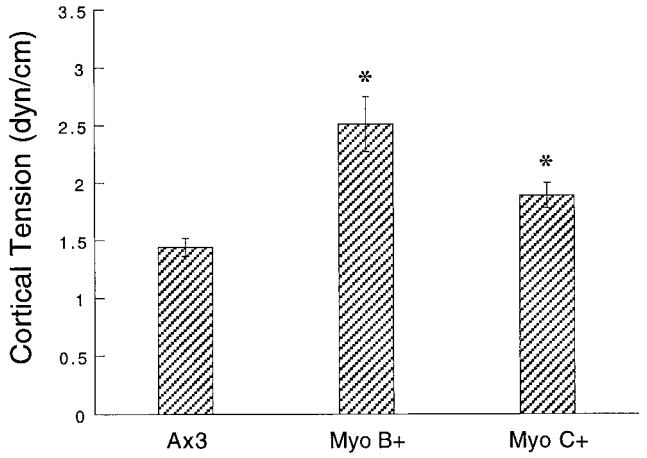

FIGURE 8 The cortical tension of the myosin I overexpression strains is increased. Shown are the results of the cortical tension measurement for two different myosin I overexpression mutants, myoB$^+$ and myoC$^+$. The average results ± standard errors for 20–50 cells in each group are shown. The * above individual bars indicates that there is a statistically significant difference between this group and the wild-type control.

ConA stimulates cortical tension in myosin I mutants

Treatment of cells with the lectin conA results in the cross-linking and capping of cell surface receptors that is accompanied by an increase in cellular cortical tension (Pasternak and Elson, 1985; Pasternak et al., 1989; Egelhoff et al., 1996). This conA-dependent increase in cortical tension has been shown to be largely dependent on myosin II in *Dictyostelium* based on the analysis of tension in several different *Dictyostelium* myosin II mutants (Pasternak et al., 1989; Egelhoff et al., 1996). The possible contribution of myosin I to the cellular response to conA was tested in both a myosin I double mutant (*myoA*$^-$/*B*$^-$) and a myosin I overexpression strain (myoB$^+$). Treatment of wild-type *myoA*$^-$/*B*$^-$ cells with conA for 30 min resulted in a significant increase in cortical tension (Fig. 9), indicating that myosin I does not contribute to conA-stimulated cortical tension in *Dictyostelium*. The level of tension observed in the myoB$^+$ overexpression mutant (Fig. 8) was greater than that observed for the control Ax3 cells. The significant increase in cortical tension in the conA-treated myoB$^+$ cells (Fig. 8) indicates that there is not an apparent threshold of overall cortical tension. These cells are capable of independently generating additional tension by stimulating myosin II-based contraction.

DISCUSSION

All cells exhibit a resting cortical tension, and increases and decreases in cortical tension are postulated to play a role in

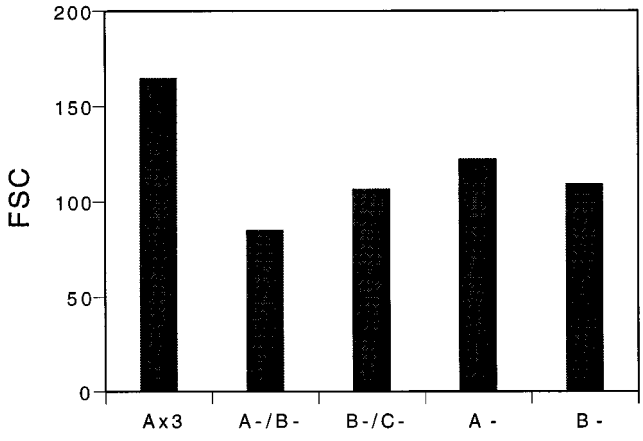

FIGURE 7 The size of the myosin I mutants is altered. Forward light scattering (FSC) was used to estimate the size of a population of cells. A total of 10^5 cells from each group were measured by FACS.

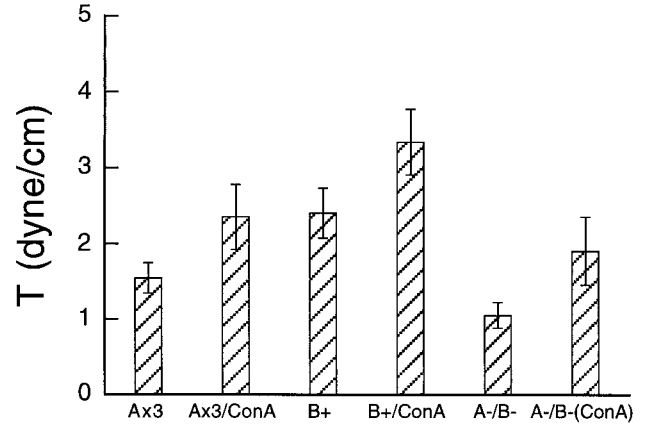

FIGURE 9 Cortical tension increases in myosin I mutants after conA treatment. Shown are the results of the cortical tension measurement for wild-type cells (Ax3) and two different myosin I mutant strains, a myosin I double mutant (*myoA*$^-$/*B*$^-$; A$^-$/B$^-$), and an overexpression strain, myoB$^+$ (B$^+$) in the absence or presence (ConA) of conA for 30 min. The average results ± standard errors for 20–50 cells in each group are shown.

cell locomotion and endocytosis (Evans, 1993; Sheetz and Dai, 1996). Cortical tension requires an intact actin cytoskeleton (Tsai et al., 1994) and may result from a combination of the contractile activity of myosin and the cross-linking of the actin by a variety of actin-binding proteins. The largest contribution appears to be provided by myosins, as deletion of either myosin II alone or two myosin I's in combination results in a loss of 50% of the resting cortical tension in *Dictyostelium* (Fig. 6; Pasternak et al., 1989), suggesting that the loss of these different myosins all together would result in a near 100% loss of cortical tension. Cortical tension is not simply the result of the myosins acting as simple actin-cross-linking proteins themselves, but rather appears to require the actual motor function (and presumably contractile activity), based on the observation that a myosin I lacking the consensus serine (S332; Novak and Titus, 1998) that is necessary for activation does not rescue the loss of cortical tension in a myosin I double mutant (Fig. 6).

The increased frequency of pseudopod formation observed in the *myoA*$^-$ and *myoB*$^-$ mutants (Wessels et al., 1991, 1996; Titus et al., 1993) is not associated with a decrease in the resting cortical tension (Fig. 6). The same amount of cortical tension is observed in the two affected myosin I single mutants. Therefore, the defects in pseudopod formation observed in the *myoA*$^-$ and *myoB*$^-$ mutants cannot be simply attributed to a loss of cortical tension. However, a significant decrease in cortical tension is observed in cells lacking two myosin I's, *myoA*$^-$/*B*$^-$ and *myoB*$^-$/*C*$^-$, revealing that the myosin I's in combination make a significant contribution to cortical tension (Fig. 6).

The observed cooperative loss of cortical tension (Fig. 6) is accompanied by a decrease in macropinocytic activity (Novak et al., 1995). The three myosin I single mutants have normal rates of macropinocytosis, whereas the *myoA*$^-$/*B*$^-$ and *myoB*$^-$/*C*$^-$ strains exhibit a significant decrease in macropinocytic activity (Novak et al., 1995). These findings suggest that the cooperative loss of cortical tension in the myosin I double mutants interferes with the effective manipulation of actin-rich macropinocytic ruffles. Consistent with this observed correlation between macropinocytosis and cortical tension, cells overexpressing either myoB or myoC exhibit both a significant increase in cortical tension and a decrease in macropinocytosis (Figs. 2 and 8; Novak and Titus, 1997). Thus, either increasing or decreasing the overall level of tension profoundly affects macropinocytosis in *Dictyostelium*. Therefore, a finely tuned balance of cortical forces seems to be required to achieve optimal uptake of fluids from the extracellular medium.

Dictyostelium cells that overexpress either myoB or myoC exhibit significant delays in streaming, consistent with lower overall rates of translocation (Fig. 2; Jung and Hammer, 1990; Wessels et al., 1991; Novak and Titus, 1997). Interestingly, the resting cortical tension of both strains is significantly increased when compared to wild-type cells (Fig. 8). Thus, whereas a decrease in cortical tension is not always accompanied by a decrease in cell motility, a significant increase in cortical tension appears to substantially reduce the ability of the cell to move. This is likely to be due to an inability of the mutant cells to efficiently extend pseudopodia due to increased cross-linking of the cortical actin cytoskeleton by myosin I.

How might the myosin I's contribute to the generation of cortical tension at the molecular level? Both myoB and myoC possess an ATP-insensitive actin-binding site in their tail regions (Pollard et al., 1991; Jung and Hammer, 1994; Rosenfeld and Rener, 1994), and it is possible that both of these myosin I's are targeted to the actin-rich cortex of the cell, where they bind to one actin filament via the ATP-insensitive actin-binding site and generate tension in the cortex by the action of the motor domain pulling on an adjacent actin filament. The mechanism by which myoA contributes to cortical tension is less clear, as it lacks a C-terminal ATP-insensitive actin-binding site (Titus et al., 1989) and is not obviously capable of cross-linking actin filaments. Given that the phenotype of mutants lacking myoA strongly resembles that of the *myoB*$^-$ mutant, it is likely that myoA must also be present in the actin-rich cortex of the cell. It may contribute to the cross-linking of filaments by being anchored to actin filaments via a mechanism different from that of myoB and myoC. A detailed analysis of the biochemical properties of the different myosin Is coupled with an examination of their functionally important domains may help to elucidate how myosin I contributes to the generation of cortical tension.

The authors thank Drs. Kris Novak and Shunji Senda for providing most of the strains used in this study and for advising us on their handling. We also thank Dr. Graham Côté (Queens University) for his generous gift of myoC antisera.

This work was supported by grants from the National Institutes of Health to MAT (GM-46486), RMH (HL-23728), and MPS (GM36277).

REFERENCES

Adams, R. J., and T. D. Pollard. 1989. Binding of myosin I to membrane lipids. *Nature.* 340:565–568.

Brzeska, H., and E. D. Korn. 1996. Regulation of class I and class II myosins by heavy chain phosphorylation. *J. Biol. Chem.* 271: 16983–16986.

Coluccio, L. M. 1997. Myosin I. *Am. J. Physiol.* 273:C347–C359.

Doberstein, S. K., and T. D. Pollard. 1992. Localization and specificity of the phospholipid and actin binding sites on the tail of *Acanthamoeba* myosin IC. *J. Cell Biol.* 117:1241–1249.

Egelhoff, T. T., T. V. Naismith, and F. V. Brozovich. 1996. Myosin-based cortical tension in *Dictyostelium* resolved into heavy and light chain-regulated components. *J. Muscle Res. Cell Motil.* 17:269–274.

Evans, E. 1993. New physical concepts for cell amoeboid motion. *Biophys. J.* 64:1306–1322.

Evans, E., and A. Yeung. 1989. Apparent viscosity and cortical tension of blood granulocytes determined by micropipette aspiration. *Biophys. J.* 56:151–160.

Faix, J., G. Gerisch, and A. A. Noegel. 1992. Overexpression of the csA cell adhesion molecule under its own cAMP-regulated promoter impairs morphogenesis in *Dictyostelium. J. Cell Sci.* 102:203–214.

Hacker, U., R. Albrecht, and M. Maniak. 1997. Fluid-phase uptake by macropinocytosis in *Dictyostelium. J. Cell Sci.* 110:105–112.

Howard, P. K., K. G. Ahern, and R. A. Firtel. 1988. Establishment of a transient expression system for *Dictyostelium discoideum. Nucleic Acids Res.* 16:2613–2623.

Jung, G., and J. A. Hammer, III. 1990. Generation and characterization of *Dictyostelium* cells deficient in a myosin I heavy chain isoform. *J. Cell Biol.* 110:1955–1964.

Jung, G., and J. A. Hammer, III. 1994. The actin binding site in the tail domain of *Dictyostelium* myosin IC (myoC) resides within the glycine- and proline-rich sequence (tail homology 2). *FEBS Lett.* 342:197–202.

Jung, G., X. Wu, and J. A. Hammer, III. 1996. *Dictyostelium* mutants lacking multiple classic myosin I isoforms reveal combinations of shared and distinct functions. *J. Cell Biol.* 133:305–323.

Kuspa, A., and W. F. Loomis. 1992. Tagging developmental genes in *Dictyostelium* by restriction enzyme-mediated integration of plasmid DNA. *Proc. Natl. Acad. Sci. USA.* 89:8803–8807.

Lee, S. F., and G. P. Côté. 1993. Isolation and characterization of three *Dictyostelium* myosin-I isozymes. *J. Biol. Chem.* 268:20923–20929.

Lynch, T. J., J. P. Albanesi, E. D. Korn, E. A. Robinson, B. A. Bowers, and H. Fujisaki. 1986. ATPase activities and actin binding properties of subfragments of *Acanthamoeba* myosin IA. *J. Biol. Chem.* 261: 17156–17262.

McNeil, P. L., A. L. Kennedy, A. S. Waggoner, D. L. Taylor, and R. F. Murphy. 1985. Light-scattering changes during chemotactic stimulation of human neutrophils: kinetics followed by flow cytometry. *Cytometry.* 6:7–12.

Miyata, H., B. Bowers, and E. D. Korn. 1989. Plasma membrane association of *Acanthamoeba* myosin I. *J. Cell Biol.* 109:1519–1528.

Mooseker, M. S., and R. E. Cheney. 1995. Unconventional myosins. *Annu. Rev. Cell Dev. Biol.* 11:633–675.

Needham, D., and R. M. Hochmuth. 1990. Rapid flow of passive neutrophils into a 4 μm pipet and measurement of cytoplasmic viscosity. *J. Biomech. Eng.* 112:269–276.

Novak, K. D., M. D. Peterson, M. C. Reedy, and M. A. Titus. 1995. *Dictyostelium* myosin I double mutants exhibit conditional defects in pinocytosis. *J. Cell Biol.* 131:1205–1221.

Novak, K. D., and M. A. Titus. 1997. Myosin I overexpression impairs cell migration. *J. Cell Biol.* 136:633–648.

Novak, K. D., and M. A. Titus. 1998. The myosin I SH3 domain and TEDS rule phosphorylation site are required for in vivo function. *Mol. Biol. Cell.* 9:75–88.

Pasternak, C., and E. L. Elson. 1985. Lymphocyte mechanical response triggered by cross-linking of surface receptors. *J. Cell Biol.* 100: 860–872.

Pasternak, C., J. A. Spudich, and E. L. Elson. 1989. Capping of surface receptors and concomitant cortical tension are generated by conventional myosin. *Nature.* 341:549–551.

Patterson, B., and J. A. Spudich. 1995. A novel positive selection for identifying cold-sensitive myosin II mutants in *Dictyostelium. Genetics.* 140:505–515.

Peterson, M. D., K. D. Novak, M. C. Reedy, J. I. Ruman, and M. A. Titus. 1995. Molecular genetic analysis of myoC, a *Dictyostelium* myosin I. *J. Cell Sci.* 108:1093–1103.

Pollard, T. D., S. K. Doberstein, and H. G. Zot. 1991. Myosin I. *Annu. Rev. Physiol.* 53:653–681.

Pollard, T. D., and E. D. Korn. 1973. *Acanthamoeba* myosin. I. Isolation from *Acanthamoeba castellanii* of an enzyme similar to muscle myosin. *J. Biol. Chem.* 248:4682–4690.

Rauchenberger, R., U. Hacker, J. Murphy, J. Niewöhner, and M. Maniak. 1997. Coronin and vacuolin identify consecutive stages of a late, actin-coated endocytic compartment in *Dictyostelium. Curr. Biol.* 7:215–218.

Rosenfeld, S. S., and B. Rener. 1994. The GPQ-rich segment of *Dictyostelium* myosin IB contains an actin binding site. *Biochemistry.* 33: 2322–2328.

Sheetz, M. P., and J. Dai. 1996. Modulation of membrane dynamics and cell motility by membrane tension. *Trends Cell Biol.* 6:85–89.

Spudich, J. A. 1982. *Dictyostelium discoideum*: methods and perspectives for the study of cell motility. *Methods Cell Biol.* 25:359–364.

Temesvari, L. A., J. M. Bush, M. D. Peterson, K. D. Novak, M. A. Titus, and J. A. Cardelli. 1996. Examination of the endosomal and lysosomal pathways in *Dictyostelium discoideum* myosin I mutants. *J. Cell Sci.* 109:663–673.

Ting-Beall, H. P., A. S. Lee, and R. M. Hochmuth. 1995. Effect of cytochalasin D on the mechanical properties and morphology of passive human neutrophils. *Ann. Biomed. Eng.* 23:666–671.

Titus, M. A., H. M. Warrick, and J. A. Spudich. 1989. Multiple actin-based motor genes in *Dictyostelium. Cell Regul.* 1:55–63.

Titus, M. A., D. Wessels, J. A. Spudich, and D. Soll. 1993. The unconventional myosin encoded by the *myo*A gene plays a role in *Dictyostelium* motility. *Mol. Biol. Cell.* 4:233–246.

Tsai, M. A., R. S. Frank, and R. E. Waugh. 1994. Passive mechanical behavior of human neutrophils: effect of cytochalasin B. *Biophys. J.* 66:2166–2172.

Uyeda, T. Q. P., and M. A. Titus. 1997. The myosins of *Dictyostelium. In Dictyostelium*: A Model System for Cell and Developmental Biology. University Academy Press, Tokyo, Japan. 43–64.

Wang, Z. Y., F. Wang, J. R. Sellers, E. D. Korn, and J. A. Hammer, III. 1998. Analysis of the regulatory phosphorylation site in *Acanthamoeba* myosin IC using site-directed mutagenesis. *Proc. Natl. Acad. Sci. USA.* 95:15200–15205.

Wessels, D., J. Murray, G. Jung, J. A. Hammer, III, and D. R. Soll. 1991. Myosin IB null mutants of *Dictyostelium* exhibit abnormalities in motility. *Cell Motil. Cytoskeleton.* 20:301–315.

Wessels, D., M. A. Titus, and D. R. Soll. 1996. A *Dictyostelium* myosin I plays a crucial role in regulating the frequency of pseudopods formed on the substratum. *Cell Motil. Cytoskeleton.* 33:64–79.

Xu, P., K. I. Mitchelhill, B. Kobe, B. E. Kemp, and H. G. Zot. 1997. The myosin I binding protein Acan125 binds the SH3 domain and belongs to the superfamily of leucine-rich repeat proteins. *Proc. Natl. Acad. Sci. USA.* 94:3685–3690.

Yeung, A., and E. Evans. 1989. Cortical shell-liquid core model for passive flow of liquid-like spherical cells into micropipets. *Biophys. J.* 56: 139–149.

Zhelev, D., and R. M. Hochmuth. 1995. Mechanically stimulated cytoskeleton rearrangement and cortical contraction in human neutrophils. *Biophys. J.* 68:2004–2014.

Zhelev, D. V., D. Needham, and R. M. Hochmuth. 1994. Role of the membrane cortex in neutrophil deformation in small pipets. *Biophys. J.* 67:696–705.